Signal Processing 93 (2013) 420–431

Contents lists available at SciVerse ScienceDirect

Signal Processing

journal homepage: www.elsevier.com/locate/sigpro

Kalman filtering strategies utilizing the chattering effects of the smooth variable structure filter

M. Al-Shabi [a], S.A. Gadsden [b,*], S.R. Habibi [b]

[a] Department of Mechatronics Engineering, Philadelphia University, Amman, Jordan
[b] Department of Mechanical Engineering, McMaster University, Hamilton, ON, Canada L8S 4L7

ARTICLE INFO

Article history:
Received 31 January 2012
Received in revised form
21 July 2012
Accepted 24 July 2012
Available online 16 August 2012

Keywords:
Kalman filter
Smooth variable structure filter
State and parameter estimation
Chattering

ABSTRACT

The Kalman filter (KF) remains the most popular method for linear state and parameter estimation. Various forms of the KF have been created to handle nonlinear estimation problems, including the extended Kalman filter (EKF) and the unscented Kalman filter (UKF). The robustness and stability of the EKF and UKF can be improved by combining it with the recently proposed smooth variable structure filter (SVSF) concept. The SVSF is a predictor–corrector method based on sliding mode concepts, where the gain is calculated based on a switching surface. A phenomenon known as chattering is present in the SVSF, which may be used to determine changes in the system. In this paper, the concept of SVSF chattering is introduced and explained, and is used to determine the presence of modeling uncertainties. This knowledge is used to create combined filtering strategies in an effort to improve the overall accuracy and stability of the estimates. Simulations are performed to compare and demonstrate the accuracy, robustness, and stability of the Kalman-based filters and their combinations with the SVSF.

1. Introduction

The field of state and parameter estimation is important for scientists and engineers. In particular, the successful control of mechanical and electrical systems depends on the knowledge of the states and parameters [1]. States determine the state of operation of dynamics of a system and are estimated using filters or observers. The purpose of estimation, as described by Bar-Shalom et al. in [1], can be one of many reasons: determination of planet orbit parameters, statistical inference, aircraft traffic control system (i.e., tracking), use in control plants with uncertainties (i.e., parameter identification or state estimation), determination of model parameters (i.e., system identification), message retrieval from noisy signals (i.e., communication theory), and also signal and image processing. A filter may be used to estimate the state of a dynamic system, whether linear or nonlinear. Filters are used when the states are estimated from measured signals in the presence of noise [1,2].

Since its introduction, the Kalman filter (KF) remains the most studied and one of the most popular tools used for estimating states. It may be applied to linear dynamic systems in the presence of Gaussian white noise, and provides an elegant and statistically optimal solution by minimizing the mean-squared estimation error [3,4]. The KF assumes that the system model is known and is linear, the system and measurement noises are white, and the states have initial conditions that are modeled as random variables with known means and variances [1,5]. However, these assumptions do not always hold in real applications. If one of these assumptions is violated, the KF becomes sub-optimal and could potentially become unstable.

To reduce modeling errors effect, several techniques have been proposed. These techniques are based on increasing the

* Corresponding author.
E-mail addresses: maqas2002@yahoo.com (M. Al-Shabi), gadsden@mcmaster.ca (S.A. Gadsden), habibi@mcmaster.ca (S.R. Habibi).

0165-1684/$ - see front matter © 2012 Elsevier B.V. All rights reserved.
http://dx.doi.org/10.1016/j.sigpro.2012.07.036

a priori covariance matrix, which in turn increases the gain value and consequently emphasizes the corrective element due to filter innovations. To increase the covariance matrix a fictitious process noise is added, or a fading memory is used [5]. The KF limitation of assuming white noise can be addressed by using a Gaussian sum to approximate the probability density function (PDF) by a finite number of Gaussian PDFs [6]. Subsequently, for each Gaussian PDF, a KF is computed in parallel and the final estimate is approximated by combining the results from these filters. In an effort to further increase numerical stability, the KF has been combined with a variety of square root algorithms and methods, such as Cholesky decomposition, UD-factorization, and triangularization algorithms [7–9]. These methods are based on reformulating the KF equations to accommodate sparse matrices and avoid instability due to round off error in numerical calculation [10].

The KF is applicable to linear systems. Common and emerging methods for nonlinear estimation include: the extended Kalman filter (EKF) [10–13], the unscented Kalman filter (UKF) [14,15], the particle filter (PF) [16,17], the smooth variable structure filter (SVSF) [18–20], and the H_∞ filter [21–24]. The SVSF is a predictor–corrector filter that is based on the sliding mode control (SMC) concepts, and can be applied to both linear and nonlinear systems. It benefits from the robustness and stability of SMC [25]. This paper demonstrates that the SVSF concept can be combined with other methods (such as the EKF and UKF) to improve their performance. Previous attempts were made in combining the EKF with the SVSF, however the results were poor and the implementation was overly complex [25]. This paper utilizes the SVSF chattering concept in an easy and effective manner creating two new filtering strategies referred to as the EK-SVSF and UK-SVSF. The EKF and UKF strategies are briefly reviewed in Section 2. Sections 3 and 4 describe the SVSF. The combined methodologies involving the EKF, the UKF, and the SVSF are presented in Section 5. Application results are provided in Section 6, followed by concluding remarks.

2. Kalman filtering strategies

2.1. Extended Kalman filter

The Kalman filter (KF) is a recursive, optimal, and model-based estimator [26]. The KF is a type of predictor–corrector filter, which uses a mathematical model of the system defined by (2.1) and (2.2) to obtain an a priori estimate of the state. The KF then uses measurements and an optimal gain to refine the a priori estimates to an a posteriori form in what is referred to as the update step. The KF process and equations are given in Fig. 1.

$$x_{k+1} = F_k x_k + G_k u_k + w_k \tag{2.1}$$

$$z_{k+1} = H_{k+1} x_{k+1} + \upsilon_{k+1} \tag{2.2}$$

where F_k, G_k, and H_k are the system, input, and measurement matrices, respectively. The corresponding estimated matrices used by the filter are $\hat{F}_{k-1}$, $\hat{G}_{k-1}$, and $\hat{H}_k$, respectively. The process (system) and measurement noise vectors are defined by w_{k-1} and υ_k, respectively. The subscripts $k|k-1$ and $k|k$ represents the a priori and the a posteriori values, respectively. The KF gain is defined by K_k; and P, Q, and R are the state error, process noise, and the measurement noise covariance matrices, respectively. A full list of the nomenclature used throughout this paper may be found in Table A1.

The KF assumes that the system model is known and is linear, system and measurement noise are white, and the states have known initial conditions [3]. However, these assumptions do not always hold in real applications. If one of these assumptions is violated, the KF can potentially become unstable [27]. The KF may only be applied to linear systems. For nonlinear systems, the popular extended Kalman filter (EKF) may be used. The EKF equations are essentially the same, except the system and measurement matrices have been linearized about the previous state estimates according to a truncated Taylor series expansion. This linearization process in itself is therefore a source of uncertainty in the estimation process [28].

2.2. Unscented Kalman filter

A sigma-point Kalman filter (SPKF) draws a certain number of points, called sigma points, from the probability distribution function projected for the states. The SPKF then projects these points by using the nonlinear model of the system to obtain an a posteriori estimate for the probability distribution, thus avoiding the requirement for linearization. The SPKF is based on the weighted statistical linear regression method [29,5]. This eliminates the need for calculating the Jacobian matrices and accommodates noise distributions that are not Gaussian [30]. The unscented Kalman filter (UKF) is

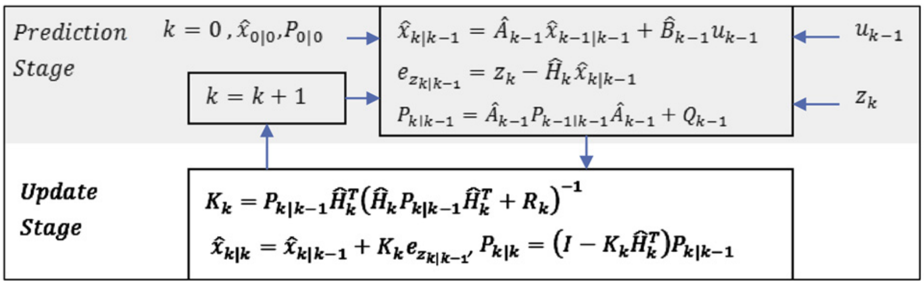

Fig. 1. Kalman filtering strategy is summarized in the above figure [5].

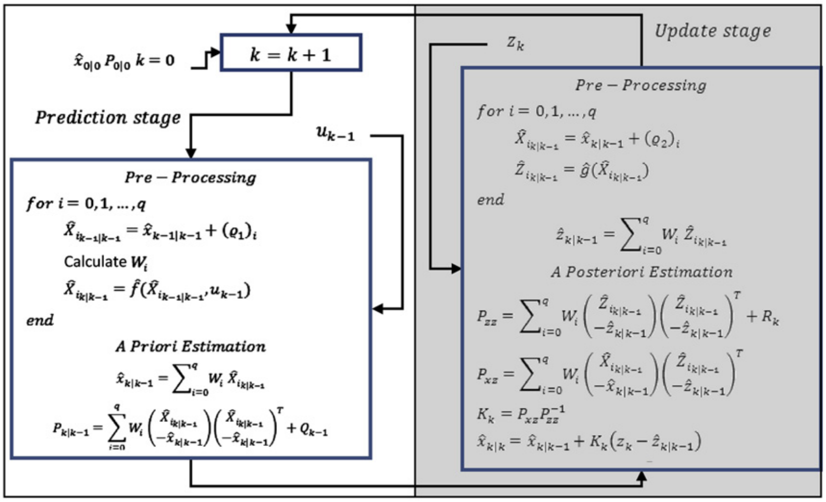

Fig. 2. Unscented Kalman filtering strategy is summarized in the above figure [5].

part of the SPKF family. The UKF obtains a minimal set of sigma points around the mean, using one of the many unscented transformations that have been proposed in the literature [5]. By propagating these points through the nonlinear system model and by using an associated weight factor, the mean and the covariance of the system are approximated. The standard UKF methodology is summarized in Fig. 2.

3. The smooth variable structure filter

The SVSF is a predictor–corrector filter that is based on SMC principles, and can be applied to both linear and nonlinear systems. A requirement of this filter is that the system needs to be differentiable, and hence the word 'smooth' is used to name this filter. The SVSF also requires that the system under consideration be observable [18,25]. The derivation of the SVSF depends on the rank of the measurement matrix (i.e., number of independent measurements compared to the number of states). If the measurement matrix has a partial rank (i.e., number of independent measurements is fewer than the number of states), then the SVSF gain is calculated using Luenberger's reduced order technique as described in [25]. Similar to the KF, the SVSF model (linear or nonlinear) is used to obtain the a priori estimate, as follows (i.e., for a nonlinear system):

$$\hat{x}_{k+1|k} = f(\hat{x}_{k|k}, u_k) \tag{3.1}$$

Utilizing the predicted state estimates $\hat{x}_{k+1|k}$, the corresponding predicted measurements $\hat{z}_{k+1|k}$ and measurement errors $e_{z_{k+1|k}}$ may be calculated:

$$\hat{z}_{k+1|k} = \hat{H}\hat{x}_{k+1|k} \tag{3.2}$$

$$e_{z_{k+1|k}} = z_{k+1} - \hat{z}_{k+1|k} \tag{3.3}$$

The SVSF then refines the a priori estimate into an a posteriori form by applying a gain as follows:

$$\hat{x}_{k+1|k+1} = \hat{x}_{k+1|k} + K_{k+1} \tag{3.4}$$

The gain used in (3.4) is defined, for a full measurement matrix, as follows:

$$K_{k+1} = H^{-1}(|e_{z_{k+1|k}}| + \gamma|e_{z_{k|k}}|) \circ \mathrm{sign}(e_{z_{k+1|k}}) \tag{3.5}$$

where γ is referred to as the SVSF 'memory' and is in the range $0 < \gamma < 1$. The gain defined in (3.5) is a function of the a priori and the previous time-step's a posteriori measurement errors $e_{z_{k+1|k}}$ and $e_{z_{k|k}}$, respectively. The a posteriori estimated measurement (3.6) is used to find the a posteriori measurement error (3.7):

$$\hat{z}_{k+1|k+1} = \hat{H}\hat{x}_{k+1|k+1} \tag{3.6}$$

$$e_{z_{k+1|k+1}} = z_{k+1} - \hat{z}_{k+1|k+1} \tag{3.7}$$

The SVSF has two sets of indicators of performance associated with each state. The primary indicators of performance are the estimated errors, and the secondary indicators of performance are chattering signals resulting from the application of the discontinuous gains. This gives the SVSF the ability to explicitly point out and extract information on modeling uncertainties. The SVSF is a robust recursive predictor–corrector estimation method that can effectively deal with uncertainties associated with initial conditions and modeling errors. It guarantees bounded-input bounded-output (BIBO) stability and the convergence of the estimation process by using the Lyapunov stability condition. The derivation of SVSF gain and its stability conditions can be found in [25] and are summarized in the following two subsections.

3.1. SVSF proof of stability

As defined in [25], let M_k be a Lyapunov function defined in terms of the a posteriori estimation error, such that:

$$M_k = |e_{z_{k|k}}| > 0 \tag{3.8}$$

The estimation process is stable if the following is satisfied:

$$M_k \Delta M_k < 0 \tag{3.9}$$

where ΔM_k represents the change in the Lyapunov function, and in this case, is defined as follows:

$$\Delta M_k = |e_{z_{k|k}}| - |e_{z_{k-1|k-1}}| \tag{3.10}$$

Substitution of (3.10) into (3.9), and rearranging, yields the following:

$$e_{z_{k|k}} \circ e_{z_{k|k}} < e_{z_{k-1|k-1}} \circ e_{z_{k-1|k-1}} \tag{3.11}$$

Eq. (3.11) is equivalent to the following, which is the stability condition for the SVSF [25]:

$$|e_{z_{k|k}}| < |e_{z_{k-1|k-1}}| \tag{3.12}$$

To remove the absolute operator in (3.12), both sides are expressed in the form of diagonal matrices (i.e., diag(e)), and are multiplied by their respective transpose, as follows:

$$\text{diag}(e_{z_{k|k}})\text{diag}(e_{z_{k|k}})^T < \text{diag}(e_{z_{k-1|k-1}})\text{diag}(e_{z_{k-1|k-1}})^T \tag{3.13}$$

Assuming that the measurement function is well-defined, constant, and linear; then from (2.1), the a posteriori measurement error may be calculated as:

$$e_{z_{k|k}} = He_{x_{k|k}} + v_k \tag{3.14}$$

Substitution of (3.14) into (3.13) yields:

$$\begin{pmatrix} \text{diag}(He_{x_{k|k}})\text{diag}(He_{x_{k|k}}) \\ +\text{diag}(v_k)\text{diag}(v_k) \\ +\text{diag}(He_{x_{k|k}})\text{diag}(v_k) \\ +\text{diag}(v_k)\text{diag}(He_{x_{k|k}}) \end{pmatrix} < \begin{pmatrix} \text{diag}(He_{x_{k-1|k-1}})\text{diag}(He_{x_{k-1|k-1}}) \\ +\text{diag}(v_{k-1})\text{diag}(v_{k-1}) \\ +\text{diag}(He_{x_{k-1|k-1}})\text{diag}(v_{k-1}) \\ +\text{diag}(v_{k-1})\text{diag}(He_{x_{k-1|k-1}}) \end{pmatrix} \tag{3.15}$$

If the measurement noise is stationary white, then by taking the expectation of both sides in (3.15) and simplifying yields the following:

$$E\begin{bmatrix} \text{diag}(He_{x_{k|k}})\text{diag}(He_{x_{k|k}}) \\ +\text{diag}(v_k)\text{diag}(v_k) \end{bmatrix} < E\begin{bmatrix} \text{diag}(He_{x_{k-1|k-1}})\text{diag}(He_{x_{k-1|k-1}}) \\ +\text{diag}(v_{k-1})\text{diag}(v_{k-1}) \end{bmatrix} \tag{3.16}$$

where $E\left[\text{diag}\left(He_{x_{k|k}}\right)\text{diag}(v_k)\right]$ and $E[\text{diag}(v_k)\text{diag}(He_{x_{k|k}})]$ vanish due to the white noise assumption. For a diagonal, positive and time-invariant measurement matrix, (3.16) becomes:

$$E\left[\text{diag}\left(e_{x_{k|k}}\right)\text{diag}\left(e_{x_{k|k}}\right)\right] < E\left[\text{diag}\left(e_{x_{k-1|k-1}}\right)\text{diag}\left(e_{x_{k-1|k-1}}\right)\right] \tag{3.17}$$

If condition (3.12) is satisfied, then from (3.17) [25]:

$$E(|e_{x_{k|k}}|) < E(|e_{x_{k-1|k-1}}|) \tag{3.18}$$

3.2. Derivation of the SVSF gain

The SVSF gain as defined in (3.5) is derived to guarantee the stability condition of (3.12). Let γ be a diagonal positive matrix with dimensions $\gamma \in \Re^{nxn}$ and with elements less than unity (i.e., $0 < \gamma_{ii} < 1$), then:

$$\gamma|e_{z_{k-1|k-1}}| < |e_{z_{k-1|k-1}}| \tag{3.19}$$

Adding the term $|e_{z_{k|k-1}}|$ to both sides of (3.19) leads to the following:

$$\gamma|e_{z_{k-1|k-1}}| + |e_{z_{k|k-1}}| < |e_{z_{k-1|k-1}}| + |e_{z_{k|k-1}}| \tag{3.20}$$

The absolute value of the SVSF gain K_k multiplied by the measurement matrix H is set to be equal to the left-hand side of (3.20) such that:

$$|HK_k| = |e_{z_{k|k-1}}| + \gamma|e_{z_{k-1|k-1}}| \tag{3.21}$$

The sign of the gain is made equal to the sign of the a priori measurement error $e_{z_{k|k-1}}$ such that (3.21) becomes:

$$K_k = H^{-1}\left(|e_{z_{k|k-1}}| + \gamma|e_{z_{k-1|k-1}}|\right) \circ \text{sign}(e_{z_{k|k-1}}) \tag{3.22}$$

Note that the proposed gain satisfies the conditions of being larger than the a priori estimation error. By applying the gain to the a priori estimate, and by substituting (3.22) and (3.5) into (3.4), the a posteriori estimated measurement is obtained:

$$\hat{z}_k = \hat{z}_{k|k-1} + \left(|e_{z_{k|k-1}}| + \gamma|e_{z_{k-1|k-1}}|\right) \circ \text{sign}\left(e_{z_{k|k-1}}\right) \tag{3.23}$$

Subtracting the measurement z_k from both sides of (3.23) yields:

$$e_{z_{k|k}} = e_{z_{k|k-1}} + \left(|e_{z_{k|k-1}}| + \gamma|e_{z_{k-1|k-1}}|\right) \circ \text{sign}(e_{z_{k|k-1}}) \tag{3.24}$$

Eq. (3.24) may be rewritten by using $e_{z_{k|k-1}} = |e_{z_{k|k-1}}| \circ \text{sign}(e_{z_{k|k-1}})$ such that:

$$e_{z_{k|k}} = -\gamma|e_{z_{k-1|k-1}}| \circ \text{sign}(e_{z_{k|k-1}}) \tag{3.25}$$

By taking the absolute value of both sides of (3.25), the following is obtained:

$$\left\{|e_{z_{k|k}}| = \gamma|e_{z_{k-1|k-1}}|\right\} < |e_{z_{k-1|k-1}}| \tag{3.26}$$

Therefore, (3.26) proves that the error decays with time, such that (3.12) and (3.18) are satisfied and the SVSF is considered BIBO stable.

4. Exploring the effects of chattering

The SVSF forces the estimate towards the true state trajectory and then retains it within a subspace, referred to as the existence subspace. This occurs both for the a priori and for the a posteriori estimates as shown in Fig. 3. The widths of the existence subspaces are functions of the uncertainties, errors in the initial conditions and/or the modeling [31].

As shown in Fig. 4, the widths are unknown and time varying for the a priori existence subspace. The a posteriori existence subspace defines a region that surrounds and encloses the true trajectory in which the estimate may exist in its a posteriori form. Its width is equal to the difference between the width of the a priori existence subspace and the amplitude of the corrective gain, as shown in Fig. 3.

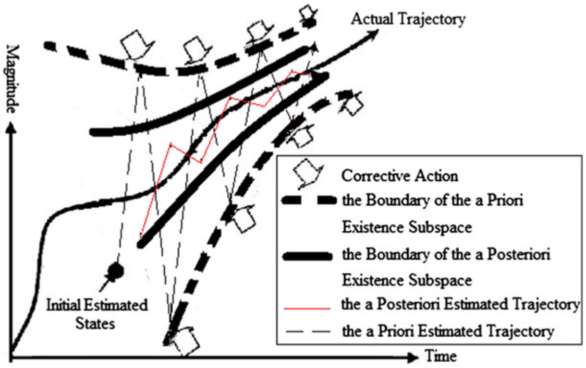

Fig. 3. Definition of the existence subspace.

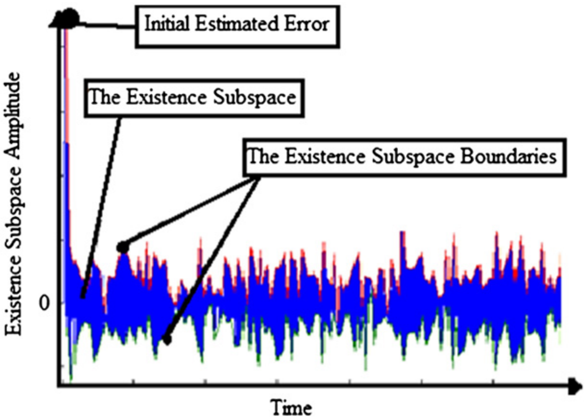

Fig. 4. Existence subspace over time.

The width of the existence subspace can be measured by using the a priori chattering signal as follows:

The a priori estimation error $e_{z_{k|k-1}}$ is defined as follows:

$$e_{z_{k|k-1}} = z_k - \hat{z}_{k|k-1} = Hx_k + v_k - \hat{H}\hat{x}_{k|k-1} \tag{4.1}$$

Using the state space model, (4.1) becomes:

$$e_{z_{k|k-1}} = H(A_{k-1}x_{k-1} + B_{k-1}u_{k-1} + w_{k-1}) - \hat{H}(\hat{A}_{k-1}\hat{x}_{k-1|k-1} + \hat{B}_{k-1}u_{k-1}) + v_k \tag{4.2}$$

Rearranging (4.2) yields:

$$e_{z_{k|k-1}} = H(A_{k-1}H^{-1}z_{k-1} - A_{k-1}H^{-1}v_{k-1} + B_{k-1}u_{k-1} + w_{k-1}) - \hat{H}(\hat{A}_{k-1}\hat{H}^{-1}\hat{z}_{k-1|k-1} + \hat{B}_{k-1}u_{k-1}) + v_k \tag{4.3}$$

where the estimated a posteriori measurement $\hat{z}_{k-1|k-1}$ is defined by:

$$\hat{z}_{k-1|k-1} = z_{k-1} + \gamma|e_{z_{k-2|k-2}}| \circ \mathrm{sgn}(e_{z_{k-1|k-2}}) \tag{4.4}$$

Substitution of (4.4) into (4.3) yields:

$$e_{z_{k|k-1}} = \begin{bmatrix} H(A_{k-1}H^{-1}z_{k-1} + B_{k-1}u_{k-1} + w_{k-1} - A_{k-1}H^{-1}v_{k-1}) + v_k \\ -\hat{H}\left(\hat{A}_{k-1}\hat{H}^{-1}z_{k-1} + \hat{B}_{k-1}u_{k-1}\right) - \hat{H}\hat{A}_{k-1}\hat{H}^{-1}\gamma|e_{z_{k-2|k-2}}| \circ \mathrm{sign}(e_{z_{k-1|k-2}}) \end{bmatrix} \tag{4.5}$$

where

$$\begin{aligned} e_{z_{k-1|k-1}} &= -\gamma|e_{z_{k-2|k-2}}| \circ \mathrm{sign}(e_{z_{k-1|k-2}}) = \\ &-\gamma|-\gamma|e_{z_{k-3|k-3}}| \circ \mathrm{sign}(e_{z_{k-2|k-3}})| \circ \mathrm{sign}(e_{z_{k-1|k-2}}) \\ &= -\gamma^2|e_{z_{k-3|k-3}}| \circ \mathrm{sign}(e_{z_{k-1|k-2}}) e_{z_{k-1|k-1}} \\ &= -\gamma^{k-1}|e_{z_{0|0}}| \circ \mathrm{sign}\left(e_{z_{k-1|k-2}}\right) \end{aligned} \tag{4.6}$$

Substitution of (4.6) into (4.5) yields:

$$\begin{aligned} e_{z_{k|k-1}} &= (HA_{k-1}H^{-1} - \hat{H}\hat{A}_{k-1}\hat{H}^{-1})z_{k-1} + (HB_{k-1} - \hat{H}\hat{B}_{k-1})u_{k-1} \\ &+ Hw_{k-1} + v_k - HA_{k-1}H^{-1}v_{k-1} \\ &- \hat{H}\hat{A}_{k-1}\hat{H}^{-1}\gamma^{k-1}|e_{z_{0|0}}| \circ \mathrm{sign}(e_{z_{k-1|k-2}}) \end{aligned} \tag{4.7}$$

The existence subspace is then obtained from the estimation error of Eq. (4.7) as follows:

$$\begin{aligned} e_{x_{k|k-1}} &= (A_{k-1}H^{-1} - H^{-1}\hat{H}\hat{A}_{k-1}\hat{H}^{-1})z_{k-1} \\ &+ (B_{k-1} - H^{-1}\hat{H}\hat{B}_{k-1})u_{k-1} + w_{k-1} - A_{k-1}H^{-1}v_{k-1} \\ &- H^{-1}\hat{H}\hat{A}_{k-1}\hat{H}^{-1}\gamma^{k-1}|e_{z_{0|0}}| \circ \mathrm{sign}(e_{z_{k-1|k-2}}) \end{aligned} \tag{4.8}$$

If no modeling errors or uncertainties are present, and the measurement matrix H is considered to be an identity matrix, then the SVSF chattering may be defined by:

$$e_{x_{k|k-1}} = -A_{k-1}v_{k-1} + w_{k-1} - \hat{A}_{k-1}\gamma^{k-1}|e_{z_{0|0}}| \circ \mathrm{sign}(e_{z_{k-1|k-2}}) \tag{4.9}$$

The a priori existence subspace represents the error in the a priori estimate. In other words, it describes the chattering of the a priori estimate around the true trajectory. In this paper, the magnitude of the resultant chattering is referred to as the a priori chattering. Due to the predictor–corrector nature of the SVSF and its gain, the a priori chattering is different from the chattering observed in other SMOs.

As mentioned earlier, the estimate has two levels of chattering: the a priori, and the a posteriori chattering. As the latter decays with time as shown by Eq. (4.6), it causes the a posteriori estimate to become more sensitive to measurement noise. In order to eliminate the a priori and the a posteriori chattering, and to reduce the sensitivity to noise, the sign function of (3.5) is replaced by a smoothing function with a known boundary layer referred to as the smoothing boundary layer, referred to as ψ. Inside the smoothing boundary layer, the corrective action is interpolated based on the ratio between the amplitude of the output's a priori estimation error and the smoothing boundary layer's width. Outside the smoothing boundary layer, the discontinuous corrective action with its full amplitude is applied. The SVSF assigns and requires one smoothing boundary layer per estimate. The following equation defines the SVSF's gain with the smoothing boundary layer:

$$K_k = \hat{H}^{-1}(|e_{z_{k|k-1}}| + \gamma|e_{z_{k-1|k-1}}|) \circ \mathrm{sat}(e_{z_{k|k-1}}, \psi) \tag{4.10}$$

where ψ is a vector consisting of smoothing boundary layer widths for each measurement, and sat is a vector of the saturation functions, defined as follows:

$$\mathrm{sat}(e_{z_{k|k-1}}, \psi) = \begin{bmatrix} \mathrm{sat}(e_{z_{1k|k-1}}, \psi_1) & \cdots & \mathrm{sat}(e_{z_{nk|k-1}}, \psi_n) \end{bmatrix}^T \tag{4.11}$$

The saturation function is defined by:

$$\text{sat}(e_{z_{ik|k-1}},\psi_i)=\begin{cases} e_{z_{ik|k-1}}/\psi_i & e_{z_{ik|k-1}}\le\psi_i \\ \text{sign}(e_{z_{ik|k-1}}) & e_{z_{ik|k-1}}>\psi_i \end{cases} \tag{4.12}$$

The smoothing boundary layer must be larger than the uncertain dynamics associated with each estimate to remove the a priori and the a posteriori chattering, and smooth the a posteriori estimate. A larger width of the boundary layer causes a slower convergence rate and degrades the filter performance as shown in Fig. 5.

If the width of the smoothing boundary layer is chosen to be larger than the width of the a priori existence subspace and the difference between them is small, then chattering is removed and the error in the output estimation is limited. When a smoothing boundary layer is used, the amplitude of the a priori chattering becomes equal to the difference between the width of the smoothing boundary layer and the output's a priori estimation error. Therefore, the width of the smoothing boundary layer determines the presence and the level of the a priori chattering. If the smoothing boundary layer is overestimated then chattering is removed. However, if due to changes in the system, additional uncertainties are added such that the amplitude of the output's a priori estimation error grows larger than the width of the smoothing boundary layer, then chattering will be observed [25,32].

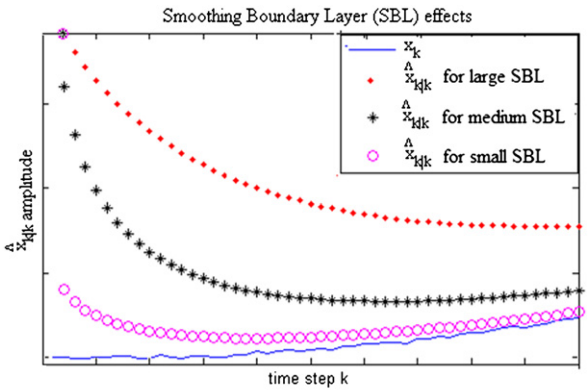

Fig. 5. Smoothing boundary layer effects over time.

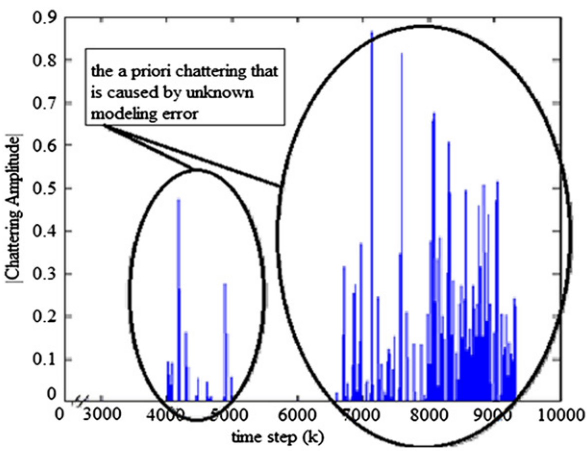

Fig. 6. Example of chattering indicator.

For example, consider the scenario shown in Fig. 6. The a priori chattering signal has been tracked for a second order system that is made to have parametric changes at time steps $t_1=4000$ and $t_2=7000$. These changes last for 1000 and 2500 time steps, respectively. The smoothing boundary layer was designed to enclose the existence subspace for the system before the parametric changes ($t<4000$ time steps). Fig. 6 shows the a priori chattering when uncertainties are injected into the model at time $t_1=4000$ and $t_2=7000$ time steps. Moreover, the figure shows the lasting period of each uncertainty injection. The SVSF is very sensitive to added uncertainties and exhibits chattering that can be used for detecting the inception of a change in the system. This capability is very useful for certain applications such as requiring early fault detection or detecting the presence of modeling uncertainties.

The smoothing boundary layer width should be defined based on Eq. (4.7) after eliminating the effect of the errors in the modeling and in the initial conditions as follows [32]:

$$\delta=|\hat{A}_{k-1}|\,|(\upsilon)_{max}|+|(w)_{max}|+|(\upsilon)_{max}| \tag{4.13}$$

If the smoothing boundary layer width is defined by (4.13); and chattering occurs, then the upper bounds are no longer valid and modeling uncertainties are present in the estimation process.

5. Combined methodologies

The SVSF may be combined with other estimation methods in an attempt to make use of the SVSF stability, and the accuracy of other methods, such as the EKF and the UKF. As such, the combined methods use the chattering equation of the regular SVSF with a constant smoothing boundary layer defined by (4.13). Outside this layer, the SVSF is dominant and its gain is used to ensure convergence to its existence subspace and stability. Thereafter, within the smoothing boundary layer, the second method (i.e., EKF or UKF) dominates the estimation process.

Note that uncertainties impact the stability of the EKF and UKF methods, as well as their performance. These filters are limited in parameter estimation applications, especially when the parameters are not constant. When a parameter changes, the covariance matrices must be updated to accommodate the change. However, the EKF and UKF methods do not have a mechanism to detect the inception of a parametric change. By combining these strategies with the SVSF, the SVSF element can be used to track changes in the system parameter. Here, the smoothing boundary layer is used to provide an upper bound on parametric uncertainties. If there is a change in a parameter and if the upper bound is reached, then chattering will result, thus indicating the inception of change in the system. Fig. 7 explains the method for combining the estimation strategies.

Essentially, when no chattering is observed, the existence subspace is within the smoothing boundary layer width where the EKF or UKF gains can be applied to update the state estimates. If a change occurs in the

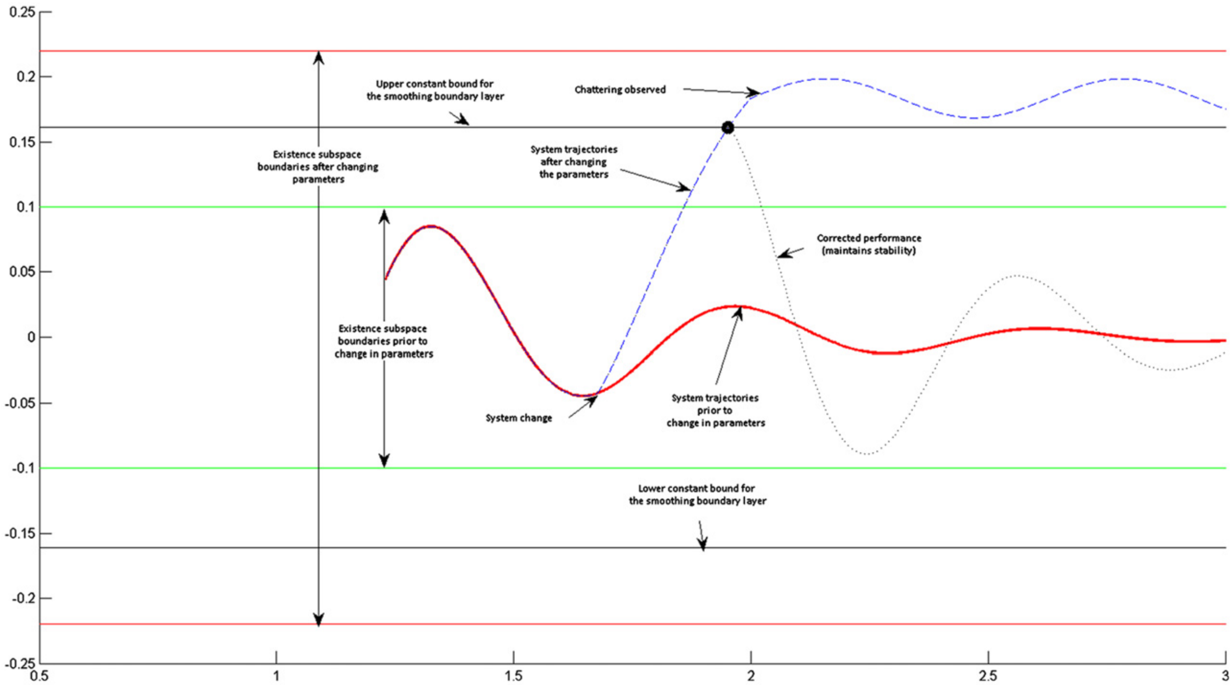

Fig. 7. Strategy for combining filtering strategies.

system, chattering is detected. The SVSF gain ensures stability by keeping it within an area of the existence subspace. The limits are set by the width of the existence subspace, which was presented earlier in the paper.

Fig. 8 illustrates the combined methods. In this paper, two methods based on the SVSF chattering are presented; the EKF-SVSF and the UKF-SVSF. The former is developed by combining the EKF with the SVSF. The EKF and SVSF strategies run simultaneous. Both methods propagate the a posteriori estimate obtained from the previous time step. If chattering is not detected in the estimation process, the EKF gain is applied. The resultant a posterior estimate and a posteriori covariance matrix are then used in the next time step. Conversely, if chattering is present, the SVSF gain is applied to the a priori estimate, and the a posteriori estimate is obtained.

First, the a priori covariance matrix is obtained as follows:

$$P_{k+1|k}=F_{k+1}P_{k|k}F_{k+1}{}^{T}+Q_{k+1} \tag{4.14}$$

where $F_{k+1}=\partial f/\partial x_{k+1|k}$. Next, the SVSF corrective gain is calculated by [28]:

$$\hat{K}_{k+1}=H^{-1}\mathrm{diag}\left[\left(|e_{z_{k+1|k}}|+\gamma|e_{z_{k|k}}|\right)\circ\mathrm{sat}\left(\overline{\psi}^{-1}e_{z_{k+1|k}}\right)\right]\mathrm{diag}(e_{z_{k+1|k}})^{-1} \tag{4.15}$$

where $\overline{\psi}^{-1}=\begin{bmatrix}\frac{1}{\psi_1} & 0 & 0\\ 0 & \ddots & 0\\ 0 & 0 & \frac{1}{\psi_m}\end{bmatrix}$. The a posteriori covariance matrix is then calculated as [28]:

$$P_{k+1|k+1}=(I-\hat{K}_{k+1}H)P_{k+1|k}(I-\hat{K}_{k+1}H)^{T}+\hat{K}_{k+1}R_{k+1}\hat{K}_{k+1} \tag{4.16}$$

The resultant a posterior estimate and a posteriori covariance matrix are then used in the next step. The UKF-SVSF has the same steps as above, except that it uses the UKF gain instead of the EKF.

6. System simulation

6.1. Description of problem

A simulation was performed to demonstrate the use of chattering to yield more accurate and stable estimates. Essentially, the presence of chattering provides an indication of modeling uncertainties or a system fault. At the presence of chattering, the estimation process is primarily transferred from the KF gain (EKF or UKF) to the SVSF gain in an effort to maintain a good estimate. The stability of the SVSF gain ensures that the estimates remain bounded to within a region of the true state trajectory.

Fig. 9A and B represent a mass-spring system used for parameter estimation in a static position and after the mass has been moved. It is assumed that the mass will not experience any angular motion, as illustrated by the connection type of the mass shown in Fig. 9B. For the purposes of this paper, it will be the goal of the filter to estimate the two stiffness parameters k_1 and k_2. This creates a rather difficult nonlinear estimation problem, which will be used to compare the filters with and without the use of SVSF chattering. From Newton's second law of motion, two sets of force equations may be found for each spring, as follows:

$$F_{1,x}=k_1\Delta r_1\cos(\theta_1) \tag{6.1}$$

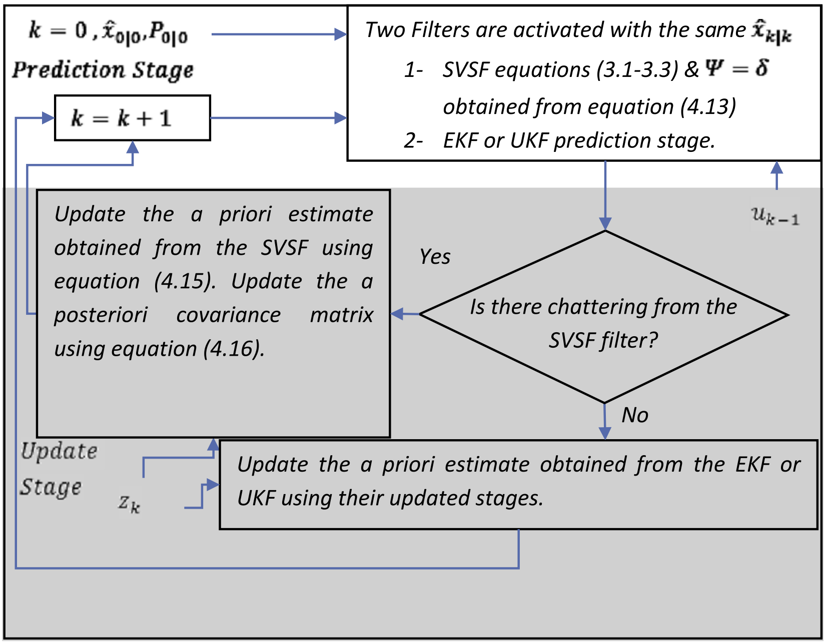

Fig. 8. The EKF-SVSF and UKF-SVSF strategies are explained in the above figure.

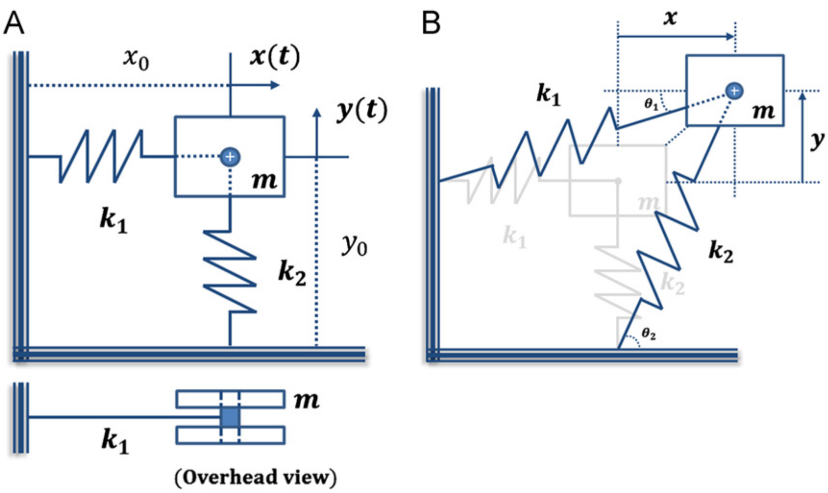

Fig. 9. (a) System in stable position. (b) System after movement.

$$F_{1,y} = k_1 \Delta r_1 \sin(\theta_1) \tag{6.2}$$

$$F_{2,x} = k_2 \Delta r_2 \cos(\theta_2) \tag{6.3}$$

$$F_{2,y} = k_2 \Delta r_2 \sin(\theta_2) \tag{6.4}$$

where Δr_i refers to the spring i elongation, and θ_i refers to the angle that each spring moves. These values are, respectively, defined as follows:

$$\Delta r_1 = \sqrt{(x_0+x)^2 + y^2} - x_0 \tag{6.5}$$

$$\Delta r_2 = \sqrt{(y_0+y)^2 + x^2} - y_0 \tag{6.6}$$

$$\theta_1 = \tan^{-1}\left(\frac{y}{x_0+x}\right) \tag{6.7}$$

$$\theta_2 = \tan^{-1}\left(\frac{x}{y}\right) \tag{6.8}$$

Note that x_0 and y_0 refer to the static position of the mass, and x and y refer to the distance moved along those respective axes, as shown in Fig. 9. Summation of the forces in both the x and y directions, yields the following two equations, respectively:

$$m\frac{d^2x}{dt^2} + k_1 \Delta r_1 \cos(\theta_1) + k_2 \Delta r_2 \cos(\theta_2) = 0 \tag{6.9}$$

$$m\frac{d^2y}{dt^2}+k_2\Delta r_2\sin(\theta_2)+k_2\Delta r_2\sin(\theta_2)=0 \tag{6.10}$$

The four kinematic states and two spring stiffness' create the state vector, defined as $\begin{bmatrix} x & \dot{x} & y & \dot{y} & k_1 & k_2 \end{bmatrix}^T$. Utilizing this notation, and (6.9) and (6.10), yields the nonlinear system equation in a discrete-time state-space format:

$$\begin{bmatrix} x_1 \\ x_2 \\ x_3 \\ x_4 \\ x_5 \\ x_6 \end{bmatrix}_{k+1} = \begin{bmatrix} x_1+Tx_2 \\ x_2-T\frac{x_5}{m}\Delta r_1\cos(\theta_1)-T\frac{x_6}{m}\Delta r_2\cos(\theta_2) \\ x_3+Tx_4 \\ x_4-T\frac{x_5}{m}\Delta r_1\sin(\theta_1)-T\frac{x_6}{m}\Delta r_2\sin(\theta_2) \\ x_5 \\ x_6 \end{bmatrix}_k + \begin{bmatrix} 0 \\ b_1 \\ 0 \\ b_2 \\ 0 \\ 0 \end{bmatrix} u_k+w_k \tag{6.11}$$

where from (6.5) through (6.8), and (6.11):

$$\Delta r_1=\sqrt{(x_0+x_1)^2+x_3^2}-x_0 \tag{6.12}$$

$$\Delta r_2=\sqrt{(y_0+x_3)^2+x_1^2}-y_0 \tag{6.13}$$

$$\theta_1=\tan^{-1}\left(\frac{x_3}{x_0+x_1}\right) \tag{6.14}$$

$$\theta_2=\tan^{-1}\left(\frac{x_1}{x_3}\right) \tag{6.15}$$

A random force of magnitude 2 N is applied to the horizontal and vertical velocities, with input gain values of $b_1=5\ \text{N}\ s/m$ and $b_2=3\ \text{N}\ s/m$. A normally distributed system noise w_k of magnitude 1×10^{-3} was applied to the states. It is assumed that Q and R are known and well-defined, and that the sensors studying the system measure range and bearing, for both position and velocity. The converted (from polar to Cartesian) measurement matrix in state-space form is as follows:

$$\begin{bmatrix} z_1 \\ z_2 \\ z_3 \\ z_4 \end{bmatrix}_{k+1} = \begin{bmatrix} \sqrt{x_1^2+x_3^2} \\ \tan^{-1}\left(\frac{x_3}{x_1}\right) \\ \sqrt{x_2^2+x_4^2} \\ \tan^{-1}\left(\frac{x_4}{x_2}\right) \end{bmatrix}_{k+1} + v_{k+1} \tag{6.16}$$

The measurement noise vector v_{k+1} is normally distributed with a magnitude of 1×10^{-3} for each measurement. In order to apply the EKF, linearized forms of the system (6.11) and measurement (6.16) equations are required. The linearized system matrix is shown in (6.17).

$$F=\begin{bmatrix} 1 & T & 0 & 0 & 0 & 0 \\ 0 & 1 & 0 & 0 & -\frac{T}{m}\Delta r_1\cos(\theta_1) & -\frac{T}{m}\Delta r_2\cos(\theta_2) \\ 0 & 0 & 1 & T & 0 & 0 \\ 0 & 0 & 0 & 1 & -\frac{T}{m}\Delta r_1\sin(\theta_1) & -\frac{T}{m}\Delta r_2\sin(\theta_2) \\ 0 & 0 & 0 & 0 & 1 & 0 \\ 0 & 0 & 0 & 0 & 0 & 1 \end{bmatrix} \tag{6.17}$$

The linearized measurement matrix H is defined as follows:

$$H=\begin{bmatrix} \frac{x_1}{\sqrt{x_1^2+x_3^2}} & 0 & \frac{x_3}{\sqrt{x_1^2+x_3^2}} & 0 & 0 & 0 \\ -\frac{x_3}{x_1^2+x_3^2} & 0 & \frac{x_1}{x_1^2+x_3^2} & 0 & 0 & 0 \\ 0 & \frac{x_2}{\sqrt{x_2^2+x_4^2}} & 0 & \frac{x_4}{\sqrt{x_2^2+x_4^2}} & 0 & 0 \\ 0 & -\frac{x_4}{x_2^2+x_4^2} & 0 & \frac{x_2}{x_2^2+x_4^2} & 0 & 0 \end{bmatrix} \tag{6.18}$$

As per the earlier discussions, it is required to transform (6.18) into a square matrix, such that 'artificial' measurements for the stiffness' k_1 and k_2 are created. A number of methods exist, such as the reduced order or Luenberger's approach, which are presented in [25,33,34]. Consider a system model involving phase variables. It is possible to derive a third 'artificial' measurement based on the available measurements. For example, suppose that one has three kinematic states, but the acceleration measurement is missing. Consider the following, where y represents an artificial measurement, let:

$$y_{3,k}=\tfrac{1}{T}(z_{2,k+1}-z_{2,k}) \tag{6.19}$$

The accuracy of (6.19) depends on the sampling rate T. In this case, applying (6.19) allows a measurement matrix equivalent to the identity matrix. The estimation process would continue as in the previous section, where a full measurement matrix was available. Note however that the artificial acceleration measurement would be delayed one time step. In this simulation, suppose that the system model (6.11) is known with complete confidence, such that it is possible to derive an artificial measurement for both stiffness values from the four available measurements. Hence, consider the following from (6.11), without knowledge of the system noise w_k:

$$x_{2,k+1}=x_{2,k}-T\frac{x_{5,k}}{m}\Delta r_{1,k}\cos(\theta_{1,k})-T\frac{x_{6,k}}{m}\Delta r_{2,k}\cos(\theta_{2,k})+b_1u_k \tag{6.20}$$

$$x_{4,k+1}=x_{4,k}-T\frac{x_{5,k}}{m}\Delta r_{1,k}\sin(\theta_{1,k})-T\frac{x_{6,k}}{m}\Delta r_{2,k}\sin(\theta_{2,k})+b_2u_k \tag{6.21}$$

Eqs. (6.20) and (6.21) may be used to solve for artificial stiffness measurements based on available measurements z_k, to be used by the SVSF for parameter estimation. Combining (6.20) and (6.21), and solving, yields:

$$\begin{bmatrix} y_{5,k} \\ y_{6,k} \end{bmatrix} = \begin{bmatrix} \frac{\Delta r_{1,k}\cos(\theta_{1,k})}{m} & \frac{\Delta r_{2,k}\cos(\theta_{2,k})}{m} \\ \frac{\Delta r_{1,k}\sin(\theta_{1,k})}{m} & \frac{\Delta r_{2,k}\sin(\theta_{2,k})}{m} \end{bmatrix}^{-1} \begin{bmatrix} \frac{b_1u_k}{T}-\frac{(z_{2,k+1}-z_{2,k})}{T} \\ \frac{b_2u_k}{T}-\frac{(z_{4,k+1}-z_{4,k})}{T} \end{bmatrix} \tag{6.22}$$

where from (6.22):

$$\Delta r_{1,k}=\sqrt{(x_0+z_{1,k})^2+z_{3,k}^2}-x_0 \tag{6.23}$$

$$\Delta r_{2,k}=\sqrt{(y_0+z_{3,k})^2+z_{1,k}^2}-y_0 \tag{6.24}$$

$$\theta_{1,k}=\tan^{-1}\left(\frac{z_{3,k}}{x_0+z_{1,k}}\right) \tag{6.25}$$

$$\theta_{2,k} = \tan^{-1}\left(\frac{z_{1,k}}{z_{3,k}}\right) \tag{6.26}$$

Note that the artificial measurements would have to be initialized (i.e., 0 is a typical value). Eq. (6.22) essentially propagates the known measurements z_k through the system model (6.11) to obtain the artificial stiffness measurements y_k. It is conceptually similar to the method presented in [25] and creates a full measurement matrix to be used in the SVSF estimation process.

6.2. Simulation results

This section provides the results of running the simulation. Fig. 10 shows the error of the x-position estimate over time. Note how the UKF and EKF methods are unable to yield very good position estimates. The SVSF is bounded closely to a region of the true state trajectory. The combination of the SVSF with the EKF and UKF allows for a more accurate state estimate. Fig. 11 further illustrates the effect of combining the SVSF with the EKF. The SVSF is bounded within a region of the position trajectory. However, the addition of the EKF further increases the accuracy, as demonstrated by the lower error amplitude.

Fig. 12 shows the true and estimated spring stiffness k_2 over time. The stiffness parameter changes two times throughout the simulation. The EKF estimate was very poor, and was omitted. Initially, the UKF had difficulty obtaining a good estimate of the parameter, but slowly converged towards a general area of the true stiffness value. However, the UKF was still unable to obtain a very good estimate. As shown Fig. 13, the SVSF chattered about the true state trajectory and then converged around the true state trajectory. The estimates from the combined methods were very good, with a limited amount of chattering.

Table 1 summarizes the overall root mean square errors (RMSE) of the filters. The EKF and UKF provided the worst estimates overall. Both methods were unable to successfully estimate the stiffness of the springs. The SVSF performed very well. However, the combined EKF-SVSF and UKF-SVSF methods provided extremely good estimates. Overall, the UKF-SVSF method performed the best

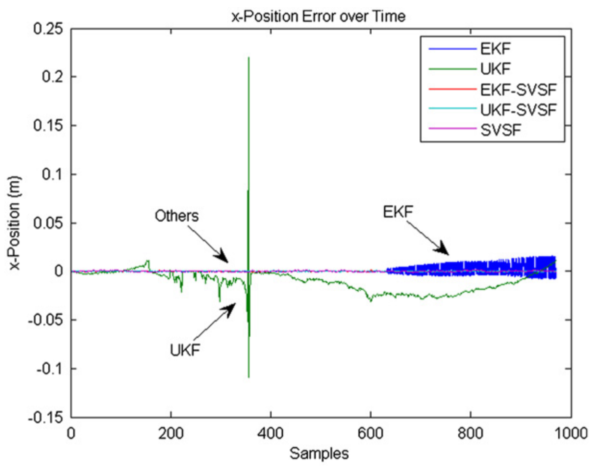

Fig. 10. Estimation results of x-position over time.

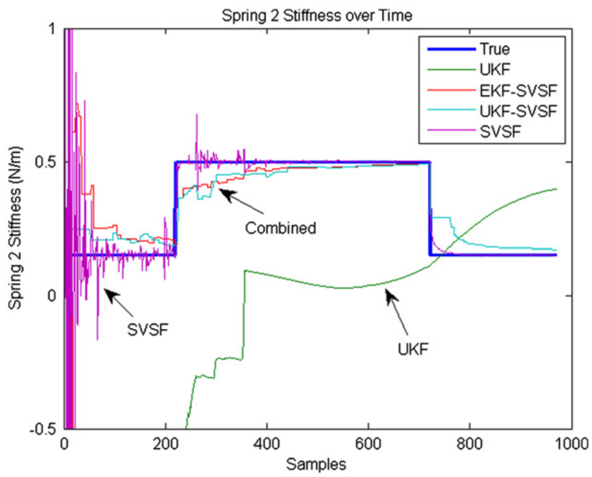

Fig. 12. Estimation of the second spring stiffness over time.

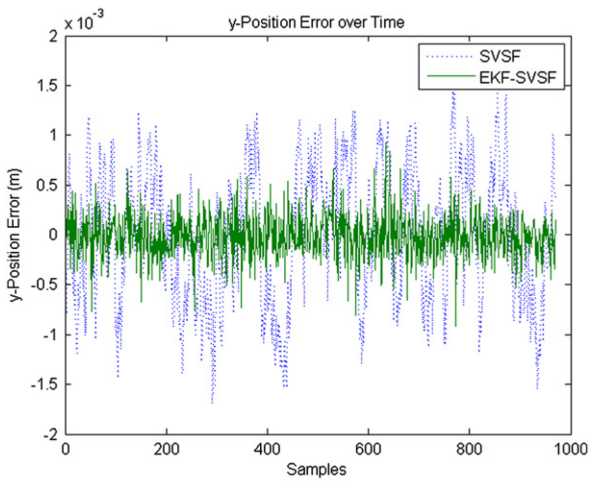

Fig. 11. Estimation results of y-position over time.

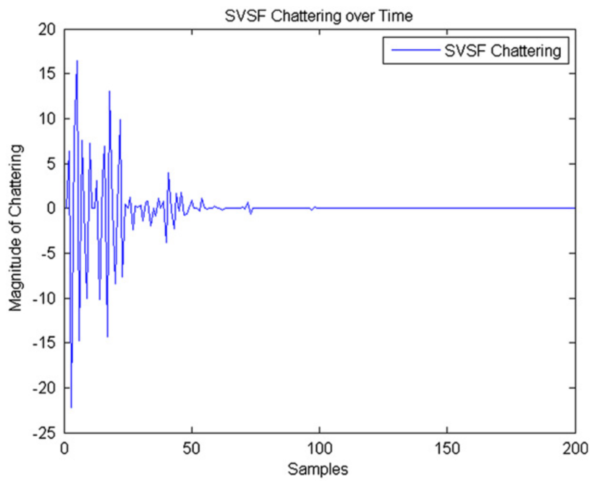

Fig. 13. Magnitude of the SVSF chattering over time.

Table 1
RMSE simulation results.

Filter	Position (m)	Velocity (m/s)	Stiffness k_1 (kN/m)	Stiffness k_2 (kN/m)
EKF	5.40×10^{-3}	4.16	106	103
UKF	3.46×10^{-2}	1.01	6.64	15.0
SVSF	8.78×10^{-4}	1.21×10^{-3}	2.05×10^{-1}	1.46×10^{-1}
EKF-SVSF	3.73×10^{-4}	6.16×10^{-3}	2.31×10^{-1}	1.68×10^{-1}
UKF-SVSF	3.76×10^{-4}	6.03×10^{-3}	1.30×10^{-1}	1.08×10^{-1}

Table A1
List of important nomenclature.

Parameter	**Definition**
X	State vector or values
Z	Measurement (system output) vector or values
Y	Artificial measurement vector or values
U	Input to the system
W	System noise vector
V	Measurement noise vector
F	Linear system transition matrix
G	Input gain matrix
H	Linear measurement (output) matrix
K	Filter gain matrix (i.e., KF or SVSF)
P	State error covariance matrix
Q	System noise covariance matrix
R	Measurement noise covariance matrix
S	Innovation covariance matrix
E	Measurement (output) error vector
$\mathrm{diag}(a)$ or $\overline{a}$	Defines a diagonal matrix of some vector a
$\mathrm{sat}(a)$	Defines a saturation of the term a
γ	SVSF 'convergence' or memory parameter
ψ	SVSF boundary layer width
$\lvert a\rvert$	Absolute value of some parameter a
$E\{\cdot\}$	Expectation of some vector or value
T	Transpose of some vector or matrix
$\hat{}$	Estimated vector or values
$k+1\vert k$	A priori time step (i.e., before applied gain)
$k+1\vert k+1$	A posteriori time step (i.e., after update)

in terms of overall accuracy and ability to estimate the stiffness of the springs.

7. Conclusions

In this paper, a relatively new estimation strategy referred to as the smooth variable structure filter (SVSF) was combined with the popular extended and unscented forms of the Kalman filter (EKF and UKF). The SVSF is a robust recursive predictor–corrector estimation method that can effectively deal with uncertainties associated with initial conditions and modeling errors. It guarantees bounded-input bounded-output (BIBO) stability and the convergence of the estimation process by using a Lyapunov stability condition. The SVSF is very sensitive to added uncertainties and exhibits chattering that can be used for detecting the inception of a change in the system. This capability is very useful for certain applications such as requiring early fault detection or the presence of modeling uncertainties. In this paper, the concept of SVSF chattering was introduced and explained. The presence of SVSF chattering was used to create two new filtering strategies, based on improving the overall accuracy and stability of the estimation process. A simulation was performed which demonstrated the effectiveness of the combined strategies.

Appendix A. List of nomenclature

The following is a table of important nomenclature used throughout this paper.

See Table A1.

References

[1] Y. Bar-Shalom, X. Rong, Li and T. Kirubarajan, Estimation with Applications to Tracking and Navigation, John Wiley & Sons, Inc., 2001.
[2] N. Nise, Control Systems Engineering, fourth ed. John Wiley and Sons, Inc, New York, 2004.
[3] B.D.O. Anderson, J.B. Moore, Optimal Filtering, Prentice-Hall, Englewood Cliffs, NJ, 1979.
[4] I. Arasaratnam, S. Haykin and R. J. Elliott,Discrete-time nonlinear filtering algorithms using Gauss–Hermite quadrature, Proceedings of the IEEE, 2007.
[5] D. Simon, Optimal State Estimation: Kalman, H [infinity] and Nonlinear Approaches, Wiley-Interscience, 2006.
[6] B. Berndt, R. Evans, K. Williams, Gauss and Jacobi Sums, John Wiley & Sons, Inc., New York, 1998.
[7] P. Kaminski, A. Bryson, S. Schmidt, Discrete square root filtering: a survey of current techniques, IEEE Transactions on Automatic Control (1971).
[8] S. Hammarling,A Survey of Numerical Aspects of Plane Rotations, 1977.
[9] H. Wang, R. Gregory, On the reduction of an arbitrary real square matrix to tridiagonal form, Mathematics of Computation 18 (87) (1964) 501–505.
[10] M.S. Grewal, A.P. Andrews, Kalman Filtering: Theory and Practice Using MATLAB, third ed. John Wiley and Sons, Inc, New York, 2008.
[11] S. Haykin, Adaptive Filter Theory, fourth ed. Prentice Hall, 2001.
[12] T. Kailath, A review of three decades of linear filtering theory, IEEE Transactions on Information Theory, Vols. IT 20 (2) (1974) 146–181.
[13] H.W. Sorenson, Least-squares estimation: from Gauss to Kalman, IEEE Spectrum (1970) 63–68.
[14] S. Julier, J. Uhlmann, H.F. Durant-White, A new method for nonlinear transformation of means and covariances in filters and estimators, IEEE Transactions on Automatic Control 45 (March 2000) 477–482.
[15] S. J. Julier, The scaled unscented transform, Proceedings of the American Control Conference, 4555–4559, May 2002.
[16] B. Ristic, S. Arulampalam, N. Gordon, Beyond the Kalman Filter: Particle Filters for Tracking Applications, Artech House, Boston, 2004.
[17] A. Doucet, N. de Freitas, N. Gordon, Sequential Monte Carlo Methods in Practice, Springer, 2000.
[18] S.R. Habibi, R. Burton, The variable structure filter, Journal of Dynamic Systems, Measurement, and Control (ASME) 125 (2003) 287–293.
[19] S.R. Habibi, The extended variable structure filter, ASME Journal of Dynamic Systems, Measurement, and Control 128 (2) (2006) 341–351.
[20] S.R. Habibi, R. Burton, Parameter identification for a high performance hydrostatic actuation system using the variable structure filter concept, ASME Journal of Dynamic Systems, Measurement, and Control (2007).
[21] M. Grimble, H_∞ fixed-lag smoothing filter for scalar systems, IEEE Transactions on Signal Processing 39 (9) (1991) 1955–1963.
[22] M. Grimble, H_∞ optimal multichannel linear deconvolution filters, predictors and smoothers, International Journal of Control 63 (1996) 519–553.
[23] T. Basar, Optimum performance levels for minimax filters, predictors and smoothers, Systems and Control Letters 16 (1991) 309–317.
[24] P.P. Khargonekar, K.M. Nagpal, Filtering and smoothing in an H_∞ setting, IEEE Transactions on Automatic Control 36 (1991) 151–166.

[25] S.R. Habibi, The smooth variable structure filter, Proceedings of the IEEE 95 (5) (2007) 1026–1059.

[26] R.E. Kalman, A new approach to linear filtering and prediction problems, ASME Journal of Basic Engineering 82 (1960) 35–45.

[27] R. Fitzgerald, Divergence of the Kalman filter, IEEE Transactions on Automatic Control (1971).

[28] S. A. Gadsden, Smooth variable structure filtering: theory and applications, Ph.D. Thesis, McMaster University, Hamilton, Ontario, 2011.

[29] S. Haykin, Kalman Filtering and Neural Networks, John Wiley and Sons, Inc., New York, 2001.

[30] X. Tang, X. Zhao and X. Zhang, The square-root spherical simplex unscented Kalman filter for state and parameter estimation, International Conference on Signal Processing Proceedings, 2008.

[31] S.R. Habibi, Parameter estimation using a combined variable structure and Kalman filtering approach, Journal of Dynamic Systems, Measurement and Control, Transactions of the ASME 130 (5) (2008) 0510041–05100414.

[32] M. Al-Shabi, The General Toeplitz/Observability Smooth Variable Structure, McMaster University, Hamilton, 2011.

[33] T. Kailath, Linear Systems, Prentice Hall, 1980.

[34] D.G. Luenberger, Introduction to Dynamic Systems, John Wiley, 1979.